Available online at www.sciencedirect.com
SCIENCE DIRECT®
ELSEVIER
International Journal of Multiphase Flow 30 (2004) 351–368
International Journal of Multiphase Flow
www.elsevier.com/locate/ijmulflow

Scaling two-phase flows to Mars and Moon gravity conditions

K.M. Hurlbert [a,*], L.C. Witte [b], F.R. Best [c], C. Kurwitz [c]

[a] NASA Johnson Space Center, Houston, TX 77058, USA
[b] Department of Mechanical Engineering, University of Houston, Houston, TX 77204, USA
[c] Department of Nuclear Engineering, Texas A&M University, College Station, TX 77843, USA

Received 22 June 2002; received in revised form 10 January 2004

Abstract

Hydrodynamic measurements are presented for two-phase flows in Mars and Moon gravity conditions. High accuracy pressure drop and flow rate data were obtained using dichlorodifluoromethane (i.e., R-12) as the working fluid flowing in a nominally 11.1 mm inner diameter tube. Measurements were made at Mars gravity, approximately 0.38-*g*, and Moon gravity, approximately 0.17-*g*, using NASA's KC-135 aircraft. A simplified scaling approach was developed using dimensional analysis and can be used to design an Earth-based test bed to simulate a Mars or Moon gravity prototype. For a specific geometry, a selected working fluid at a fixed temperature and pressure, and a particular flow regime condition, the pressure drop functional scaling equation is a simple, power-law relationship for the Euler number as a function of only the Froude number. The research completed supports the use of Earth-g tests to predict the behavior of two-phase systems for Moon-g and Mars-g applications.

Keywords: Two-phase flow; Scaling; Partial gravity; Low gravity; Mars; Moon; Annular flow; Stratified flow

1. Introduction

The National Aeronautics and Space Administration (NASA), the United States Air Force, other government agencies, and commercial and academic groups continue to pursue the development of two-phase systems for space applications in numerous areas. The NASA Johnson Space Center (JSC) specifically has an avid interest in two-phase systems for active thermal control and life support. Other areas of potential for these systems might include in-situ resource

* Corresponding author.

0301-9322/$ - see front matter © 2004 Published by Elsevier Ltd.
doi:10.1016/j.ijmultiphaseflow.2004.01.004

utilization designs for planetary missions, spacecraft using nuclear-based power generation, propellant transfer and commercial space processing.

Two-phase flows in this case are defined as those having the liquid and vapor phases of a working fluid flowing co-currently together. Two-phase systems can offer significant advantages in many space applications. One example is active thermal control, where up to an 80% savings in system power and 20% savings in mass can be realized (Ungar, 1995). Another area currently under investigation is the use of a two-phase bioreactor-based water treatment system for human space missions. The advantage of bioreactor-based systems over the physical–chemical approach is the replacement of two key components; the vapor compression distillation and ultrafiltration systems (Hanford, 1997). Therefore, potential savings are realized in system mass, power and volume, while increasing reliability and maintaining a highly efficient water treatment process.

Two-phase flow experimental studies at partial gravities have been limited, and only three researchers have previously published theories for scaling to partial-g or zero-g conditions. C. Crowley published the first work for scaling two-phase flow systems for space applications. Crowley (1991) suggested that a freon (i.e., R-11) system could be used to simulate a large-scale, microgravity, two-phase system with ammonia as its working fluid. The paper provided dimensional and non-dimensional scaling parameters for various components of a two-phase design, but a number of weaknesses were identified. Most critically, key variables were not accounted for in the scaling such as the viscosity and surface tension properties of the working fluids. A.A.M. Delil of the National Aerospace Laboratory NLR has over the last decade published numerous works for scaling two-phase systems for space applications (Delil, 1991, 1998, 1999, 2000). Delil investigated the application of the Buckingham Pi Theorem for scaling two-phase flows, which has been proven for single-phase flows. The methodology proposed by Delil (1991) was considered sound, but his published work lacked experimental data and the associated analyses to support the theory. Shortly after the initial work of Delil (1991), E.K. Ungar began investigating the use of dimensional analysis for scaling two-phase flows for specifically zero-g applications. Ungar et al. (1998) theorized that a horizontal, Earth-g, two-phase test bed could be used to simulate a zero-g, two-phase system or components if several ''gravity insensitive'' criteria were met and five independent dimensionless groups were matched simultaneously. As with Delil (1991), the use of the Buckingham Pi Theorem was considered a viable technique, but concerns were identified with the proposed approach. While other researchers (e.g., Delil, 2000) agree that the development/selection of the dimensionless parameters can be somewhat arbitrary, it was hypothesized for the current research that this selection is critical to properly describing two-phase flows for various conditions. Also, the notion of using a ground test bed to simulate zero-g, two-phase flows is attractive, but the ''gravity insensitive'' criteria presented by Ungar et al. (1998) must, as they state, be confirmed experimentally. In addition, the methodology proposed is limited to only high annular (i.e., high modified Froude number) or intermittent-type flows and horizontal configurations. A more generic approach may be needed to support various system designs.

The work presented in this paper is the first to investigate two-phase flow dynamics and scaling using validation data for Earth, Mars, and Moon gravities. First, a description of the experimental hardware and data collection is provided. Next, the scaling development is described along with the validation techniques used in this study. Finally, a summary of the findings is presented.

2. Experimental

One of the major tasks of the current research program was to obtain two-phase flow data for Earth-g and Mars-g conditions to support scaling studies. A special NASA aircraft is modified to fly parabolic trajectories to simulate zero-g or partial-g conditions. As shown in Fig. 1, a typical parabolic maneuver includes a 45-degree climb at approximately 1.8-*g*, followed by a "nose-over" at the top of the parabola where the targeted acceleration conditions are experienced, and then continuation into a 45-degree dive through a 1.8-*g* pullout.

Reduced gravity periods of approximately 20–30 seconds can be achieved during each parabolic maneuver, and a typical flight provides 40 or more parabolas. Earth-g data were obtained by performing experiments in the Interphase Transport Phenomena (ITP) Laboratory at Texas A&M University. The experiments reported here were performed from July 1999 to May 2000 using the test rig described in the following section, which was modified and maintained by Texas A&M University in cooperation with the University of Houston and the NASA Johnson Space Center.

2.1. Test rig

A schematic of the two-phase flow test bed used in the current research is shown in Fig. 2. The test rig was a modified version of that used by Miller et al. (1993), Reinarts et al. (1993), and Ungar et al. (1994). All testing, whether single or two-phase, was performed using single component, dichlorodifluoromethane (R-12). R-12 was originally chosen for this test package due to its low toxicity, low heat of vaporization, material compatibility properties, and high vapor density at acceptable pressures (Miller et al., 1993).

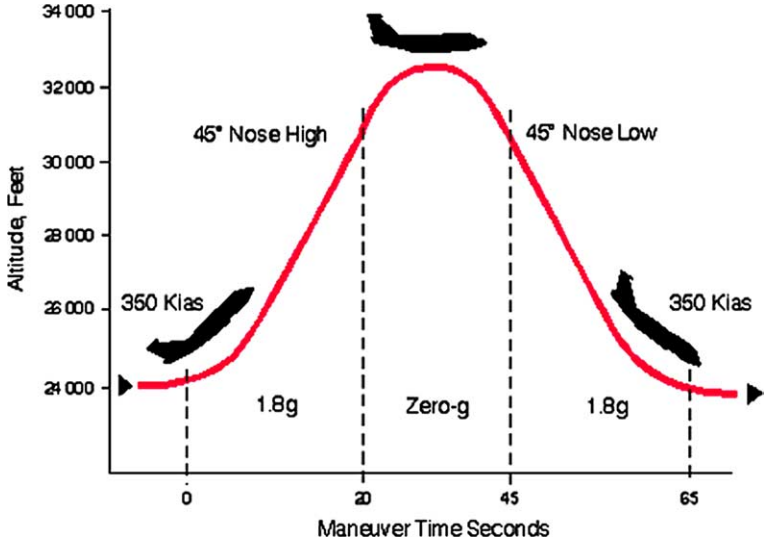

Fig. 1. Typical parabolic maneuver performed by the NASA KC-135.

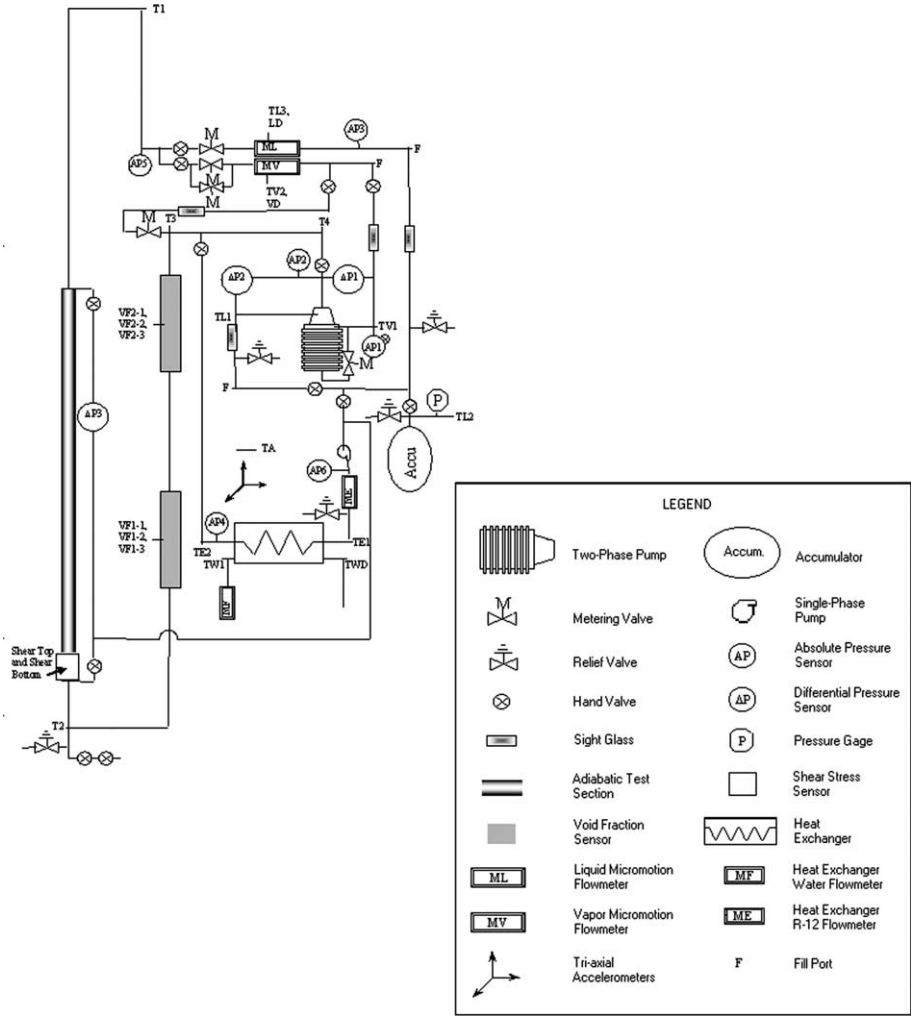

Fig. 2. Two-phase flow test bed schematic.

The ''heart'' of the test bed was the two-phase pump, which works as both a pump and phase separator. Two-phase flow entered the pump, was centrifugally separated, and then the vapor and liquid were pumped through their separate respective flow paths. This pump-accumulator allowed the flow rates of each phase of the working fluid to be controlled and measured separately, providing a highly accurate flow quality calculation as described in the following paragraph.

Mass flow rate sensors were used to accurately measure the mass flow rates of the separated liquid and vapor phases. These sensors provided measurements to within an accuracy of ±1% for the liquid flow rate over the range of the current test program and to within ±2% for the vapor phase. High accuracy in these measurements was critical to obtain an accurate mass quality calculation, which is defined as the mass rate of flow of the vapor phase divided by the total mass flow rate. Using the calculated mass quality, measured mass flow rates, computed cross sectional area, and the fluid properties, the superficial vapor and liquid velocities could then be computed

and used to determine the velocity ratio. As will be seen in Sections 3 and 4, the velocity ratio (the superficial vapor velocity divided by the superficial liquid velocity) is an important parameter in scaling from Earth-g conditions to partial gravity conditions.

The first test section downstream of the pump has historically been dedicated to adiabatic flow regime and pressure drop testing (i.e., Miller et al., 1993; Reinarts et al., 1993; Ungar et al., 1994). The test section was composed of Pyrex brand, heavy wall, glass tubing with an inner diameter of nominally 11.1 mm. The test section was oriented horizontally with respect to the Earth gravity vector, or aircraft floor for all testing. Upstream of the test section, a straight entrance/developing length of 0.78 m was provided, resulting in a length to diameter ratio (L/D) of 70. The straight exit length was minimal due to the width constraint of the KC-135 aircraft and provided only 20 L/D. During zero-g operations in the KC-135, the test bed was oriented with the test section perpendicular to the plane axis (i.e., in the wing to wing orientation). It has been shown previously that this orientation minimizes the effects of residual accelerations and results in less hydrostatic effects along the test section axis during the parabolas (Wheeler, 1992; Wheeler et al., 1993).

As in the work of Miller et al. (1993) and Ungar et al. (1994), pressure drop measurements across the adiabatic test section were taken using instrumentation described in Wheeler (1992). The sensors were calibrated at Texas A&M University for a range of 0–12.2 kPa, and had an overall accuracy of ±0.2% of the calibrated span (i.e., ±24 Pa).

Additional differential pressure instruments, pressure transducers and temperature sensors, shown in Fig. 2, were included to evaluate overall system performance and fluid conditions throughout the flow loop. A high speed imaging system was used to collect imagery data to identify flow regimes. Two void fraction sensors developed for the NASA Glenn Research Center were "piggy-backed" during the flights in a second test section to provide initial data and calibration information, and while the results of these measurements are interesting, they were not a part of the current research. The Data Acquisition and Control System (DACS) was designed and provided by Texas A&M, and was similar to the system used in earlier work (Reinarts, 1993). Finally, tri-axial acceleration measurements were made throughout the flight tests and were used to determine the accuracy of achieving the targeted acceleration level for all test points.

2.2. Data validation

There were two parts to the validation effort for the data collected in the current program. First, pre-flight and post-flight ground tests were conducted to ensure that the equipment was operating properly before and after the flight tests. These tests included single-phase flow conditions, which were used to compare the pressure drop measurements against predictions using the following equation:

$$\Delta p = f \frac{L}{D} \frac{1}{2} \rho_{\mathrm{L}} u_{\mathrm{L}}^2. \tag{1}$$

Here, Δp is the calculated pressure drop through the test section, (Pa), f is the friction factor, ρ_{L} is the liquid density, (kg/m^3), and u_{L} is the liquid flow velocity, (m/s). The Blasius friction factor correlation for a smooth tube, Eq. (2), was selected and used in Eq. (1) for the turbulent flow data obtained in ground testing,

$$f = \frac{0.3164}{Re_{\mathrm{L}}^{0.25}}, \tag{2}$$

where Re_{L} is the Reynolds number of the liquid phase only. Excellent agreement was obtained for these tests conducted throughout the program, supporting the accuracy of the pressure drop data and other measurements made in the current research.

Second, the data collected during the flight and ground tests were both qualitatively and quantitatively reviewed to ensure the quality of the measurements. Additionally, these data were classified by flow regime (i.e., the spatial orientation of the liquid and vapor phases) according to the definitions provided by Reinarts et al. (1993) as shown in Fig. 3. A complete listing of the data obtained during the Mars-g flight tests and ground tests can be found in Hurlbert (2000).

2.3. Uncertainty analysis

While the deterministic (quantifiable) errors associated with the data collected in this study based on instrument precision, digital acquisition error, etc. were relatively small, the uncertainties based on random effects were more significant because of the environmental conditions in

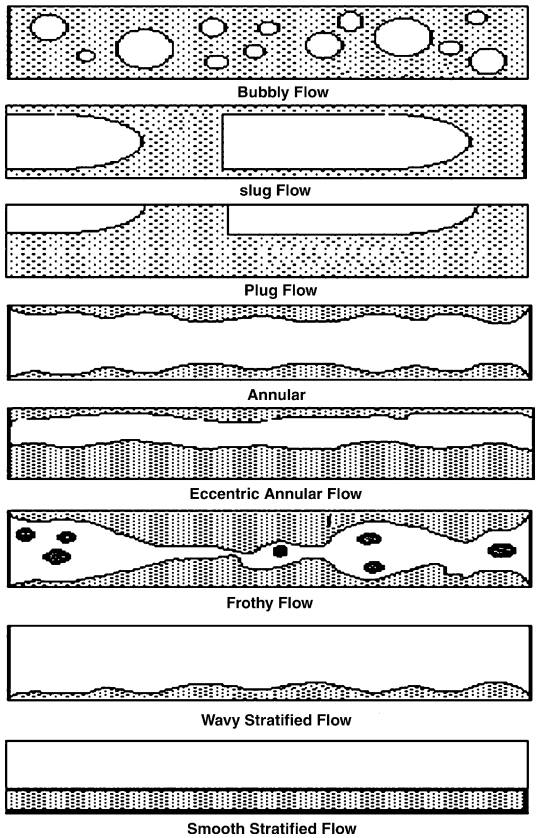

Fig. 3. Sketch of flow regimes.

the aircraft facility and associated operational issues. A detailed description of the challenging test environment of the KC-135 is included in Hurlbert (2000).

Because of the testing in the aircraft environment, the uncertainty analysis relied on the observed uncertainty or calculated standard deviation of the key measurements. The standard deviations account for the errors associated with the instrumentation, DACS, etc. and also account for the non-deterministic uncertainties that may affect the measurements through the flights. For the key measurements made during the flights, such as the pressure drop, the error was calculated as twice the standard deviation (i.e., 2σ) computed from the measurements recorded during the "steady" portion of the parabolas. Using twice the standard deviation to state the uncertainty of the data increases the probability range, and can be interpreted as providing a 95% probability that a single data point would have a deviation within $\pm 2\sigma$ about the mean value. Typical results of these computations are shown as error bars on graphs throughout this paper.

In some cases, analyses of the data required the measured values to be combined into other parameters, like the Euler number. Errors in individual measurements are propagated leading to an overall error associated with the combined parameter. The overall error/uncertainty of the combined parameter must account for the accumulation of error, and the following equations were used to account for this:

$$\frac{\delta R}{R} = \left[\sum_{i=1}^{N} \left(A_i \frac{\delta x_i}{x_i} \right)^2 \right]^{1/2}, \tag{3}$$

where

$$R = x_1^{A_1} x_2^{A_2} \ldots x_N^{A_N}. \tag{4}$$

Here, R represents the combined parameter and is a product function of the measured values (i.e., x_i values). The δx_i values in Eq. (3) are the errors of the individual measurements, which were calculated as 2σ as described previously. Again, typical error/uncertainty values were computed and are shown as error bars on some graphs in this paper.

3. Scaling theory

The pressure drop in plumbing lines is of key interest in designing two-phase systems. Accurate pressure drop predictions allow for sizing of pump(s) and determination of the required operational power. Mass, volume, and power are critical for space systems because of high launch costs and severe limitations on power consumption. Therefore, Eq. (5) was derived using dimensional analysis applied to the dimensional quantities of interest for two-phase flows:

$$Eu_{\mathrm{L}} = \mathrm{fn}\left(\frac{L}{D}, \frac{\varepsilon}{D}, \cos \upsilon, \frac{\rho_{\mathrm{G}}}{\rho_{\mathrm{L}}}, \frac{\mu_{\mathrm{G}}}{\mu_{\mathrm{L}}}, We_{\mathrm{L}}, Re_{\mathrm{L}}, S, Fr_{\mathrm{L}} \right). \tag{5}$$

It should be noted that Eq. (5) is valid for actively pumped two-phase systems, and may not be applicable to systems relying on capillary pumping. In Eq. (5), Eu_{L} is the Euler number of the liquid phase, L/D is the pipe length to diameter ratio, ε/D is the pipe surface roughness to diameter ratio, υ is the angle between the inertial and gravitational forces in degrees, $\rho_{\mathrm{G}}/\rho_{\mathrm{L}}$ is the gas to liquid density ratio, $\mu_{\mathrm{G}}/\mu_{\mathrm{L}}$ is the gas to liquid viscosity ratio, We_{L} is the Weber number of

the liquid phase, S is the velocity ratio (i.e., the ratio of the superficial vapor velocity to the superficial liquid velocity), and Fr_L is the Froude number of the liquid phase. By placing Eu_L on the left-hand side, a non-dimensional relationship for pressure drop can be evaluated in terms of the other dimensionless groups of interest.

For two-phase space systems, it may be difficult or impossible to match all of the non-dimensional parameters shown in Eq. (5) over a wide range of conditions. The scaling relationship developed includes nine dimensionless parameters that would have to be matched in order to achieve full similarity, including the geometry, fluid properties, flow conditions, and gravity level. Due to the testing limitations of the current research program, varying most of these parameters was not possible. Therefore, a simplified approach was adopted.

First, the layout of the test section for the current experiment was identical to earlier tests completed by Ungar et al. (1994). This allowed for the elimination of the dimensionless geometry parameters (i.e., L/D, ε/D, and υ) from scaling consideration. The fluid properties were also matched by using the same working fluid and operating at the same temperature and pressure as in the earlier experiments. This approach greatly simplifies the analyses, and is considered realistic for partial-gravity systems where the actual working fluids can be used in ground test systems (e.g., air/water). The governing scaling equation, Eq. (5), then becomes

$$Eu_L = \mathrm{fn}(We_L, Re_L, S, Fr_L). \tag{6}$$

A further simplification was pursued based on the work of Jayawardena et al. (1997). The Suratman number (Su) combines the Re and We numbers into a single non-dimensional parameter,

$$Su = \frac{Re_L^2}{We_L} = \frac{\sigma \rho D}{\mu^2}. \tag{7}$$

Here, σ is the surface tension (N/m), ρ is the density (kg/m^3), D is the diameter (m), and μ is the viscosity (Ns/m^2). The resulting parameter is only a function of the fluid properties and pipe diameter, which were already matched as described previously. This simplification was also pursued based on the approach presented by Delil (1991), where combinations of dimensionless groups could be selected to suit the specific problem being investigated. However, it was noted that this technique should be undertaken with care, and could rely upon the researcher's knowledge of two-phase flows and the associated influence of important variables. An example is that use of the Suratman number may not be practical for very small diameter tubes (e.g. capillary) as surface tension plays a larger role and may dominate the flow conditions. Another caution is that the combined parameters are not truly independent and may "mask" important dependencies if all the independent variables are not preserved in the functional relationship. For the current work, use of the Suratman number was considered viable because of the size of the test section (i.e., approximately 11 mm ID) and resulted in a simpler scaling relationship,

$$Eu_L = \mathrm{fn}(S, Fr_L). \tag{8}$$

A similar simplification was realized in examining the remaining dimensionless parameters of Eq. (8), where Eu_L is the Euler number which relates pressure to inertia forces. The Buckingham Pi Theorem states that the dimensionless groups in the equation must be themselves independent of each other, and all of the independent variables must be included in these groupings. The independent variables on the right-hand-side of Eq. (8) are the superficial vapor velocity, (m/s),

the superficial liquid velocity, (m/s), gravity, (m/s^2), and diameter, (m). However, j_L is also included on the left-hand side of the equation. Again, by combining two dimensionless parameters (i.e., S and Fr_L) as suggested by Delil (1991) and demonstrated by Jayawardena et al. (1997), a single non-dimensional parameter was obtained,

$$Fr_G = \frac{Fr_L}{S^2} = \frac{j_G^2}{gD}. \tag{9}$$

The superficial liquid velocity (j_L) is preserved in the scaling equation on the left-hand side, and thus all the independent variables are still accounted for. The final result was a scaling relationship for the current work of the form

$$Eu_L = \mathrm{fn}(Fr_G). \tag{10}$$

Eq. (10) requires an identical geometry and the same working fluid (i.e. matched thermophysical properties) for each data point obtained.

4. Results

The data obtained by Ungar et al. (1994) were used as a baseline for the present research. New data obtained during KC-135 flights and ground testing were specifically targeted to duplicate the operating temperatures and pressures for both the previous Moon and Mars data. According to Eq. (10), the measured Eu_L would then only depend on the Fr_G across all flow conditions and gravity levels. However, when the data were plotted there was considerable scatter, which obscured a definitive functional relationship. Consequently, an alternative correlation technique was pursued. Rather than using single-phase (liquid) flow theory as the basis for dimensional analysis, one could start with single-phase (vapor) flow theory. Using the same assumptions and methodology described in Section 3, a scaling relationship was developed as

$$Eu_G = \mathrm{fn}(Fr_L). \tag{11}$$

The data were plotted in terms of Eu_G and Fr_L to compare with Eq. (11). Fig. 4 shows the data for the February 2000 Mars and May 2000 Earth tests. Indeed, an obvious functional relationship is observed. This approach is believed to be more accurate because the two-phase pressure drop is more sensitive to superficial vapor velocity due to the influence of vapor velocity on interfacial wave structure. However, the data indicate an interesting asymptotic behavior at very low Fr_L values (i.e., Fr_L less than approximately 0.01) and increased scatter with increasing Fr_L. The following sections explore this behavior in more detail.

4.1. Scaling at high velocity ratios

Only limited Earth gravity data were obtained in the current research for values of Fr_L less than 0.01. Fig. 4 shows that these data tend to plateau and appear to approach a constant Eu_G value as Fr_L reaches low values. An examination of the data showed a common characteristic; namely, all had very high velocity ratios (i.e., $S > 100$). An evaluation was carried out comparing the measured pressure drops to those predicted assuming single-phase, vapor flow. It was determined that

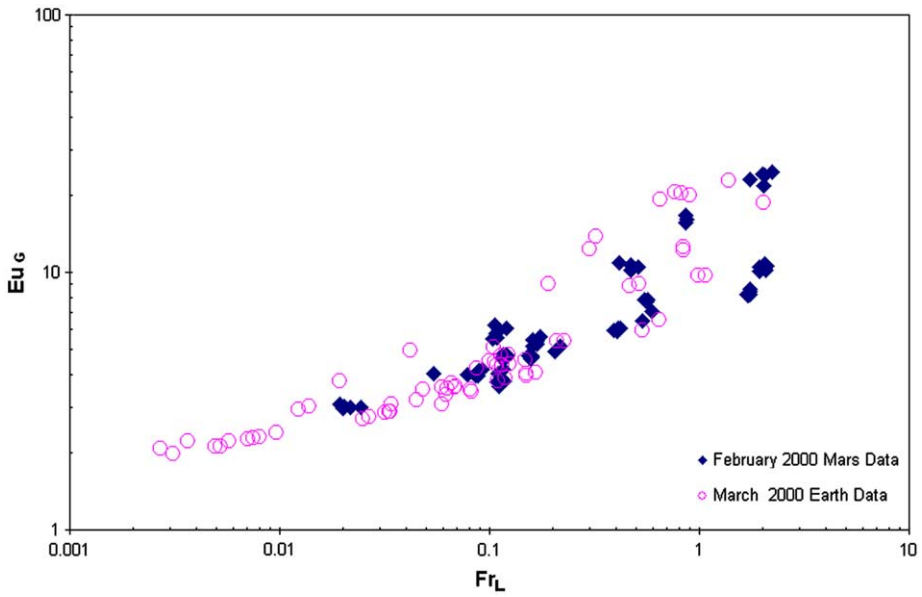

Fig. 4. Eu_G versus Fr_L for 2000 Mars and Earth data.

if the relative roughness (i.e., ε/D) of the liquid/vapor interface is known or can be predicted accurately, it may be possible to predict the pressure drops for high slip conditions based on single-phase vapor flow theory alone. Because the current research program obtained very little two-phase data at high velocity ratios, this conclusion could not be definitively substantiated but rather provided a direction for future work. These data were therefore excluded from the scaling analyses presented in the following section.

4.2. Scaling based on flow regimes

As mentioned previously, the data in Fig. 4 (for values of the Fr_L number greater than 0.01) are notably scattered. While some deviation was expected based on variations in system temperature, uncertainties in the measurements, etc., the trend implies a dependency on the independent variables (i.e., j_L, j_G, and g). An explanation for this was found in the development of the dimensionless scaling relationship. A basic premise of the current research was that two-phase flow regimes are related by the same independent variables as the pressure drop. Therefore, a non-dimensional analysis would result in the same functional equation,

$$\text{flow regime} = \text{fn}\left(\frac{L}{D}, \frac{\varepsilon}{D}, \cos\upsilon, \frac{\rho_L}{\rho_G}, \frac{\mu_L}{\mu_G}, We_G, Re_G, S, Fr_G\right). \tag{12}$$

The simplified scaling approach described in Section 3 was then thought to be independent of the flow regime, however this is not true in the last step. Eq. (8) was further simplified by using the definition of the Fr_G, and this was justified because the superficial liquid velocity was included on the left-hand side of the equation in the *Euler* number. Clearly this simplification cannot be made

for the flow regime. Therefore, the flow regime relationship can only be simplified to the following functional equation:

$$\text{flow regime} = \text{fn}(S, Fr_L), \tag{13a}$$

or, alternately

$$\text{flow regime} = \text{fn}(S, Fr_G). \tag{13b}$$

Fig. 5 clearly shows the dependency of the flow regime on S and Fr_L as stated in Eq. (13a). For a given Fr_L, eccentric annular (EA)- or annular (AN)-type flows are achieved with higher S values (i.e., eccentric annular/annular type flows are present at higher j_G values). Therefore, the scaling relationship of Eq. (11) would hold only for specific two-phase flow regimes. This can also be seen in Fig. 6, which duplicates Fig. 4 but identifies the specific regimes.

The data collected in the current research were primarily wavy stratified (WS)-type regimes and eccentric annular- or annular-type regimes. Fig. 7 shows the scaling relationship of Eq. (11) compared to the wavy stratified and wavy stratified-transition data of the current research, for $S < 100$.

A clear functional relationship is seen and the best fit of the data yields a power function of the form

$$Eu_G = 17.5 Fr_L^{0.45}. \tag{14}$$

The best-fit equations for the current research were determined by minimizing the square of the error between the measured data and the values predicted by the fitted equation. The advantages of this method are that it is simple and well understood, and a detailed description can be found in

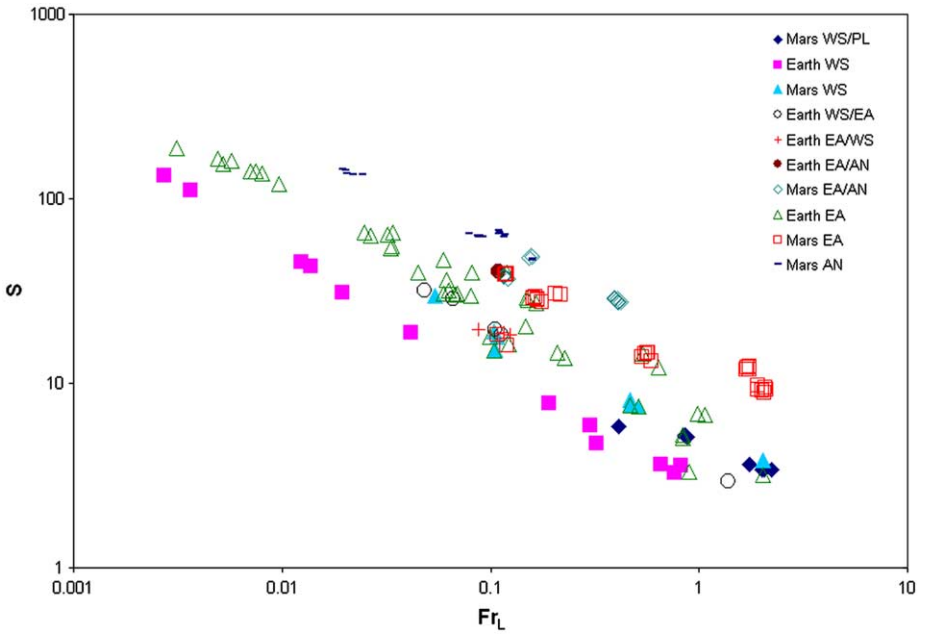

Fig. 5. Velocity ratio (S) versus Fr_L for 2000 Mars and Earth data with flow regimes specified.

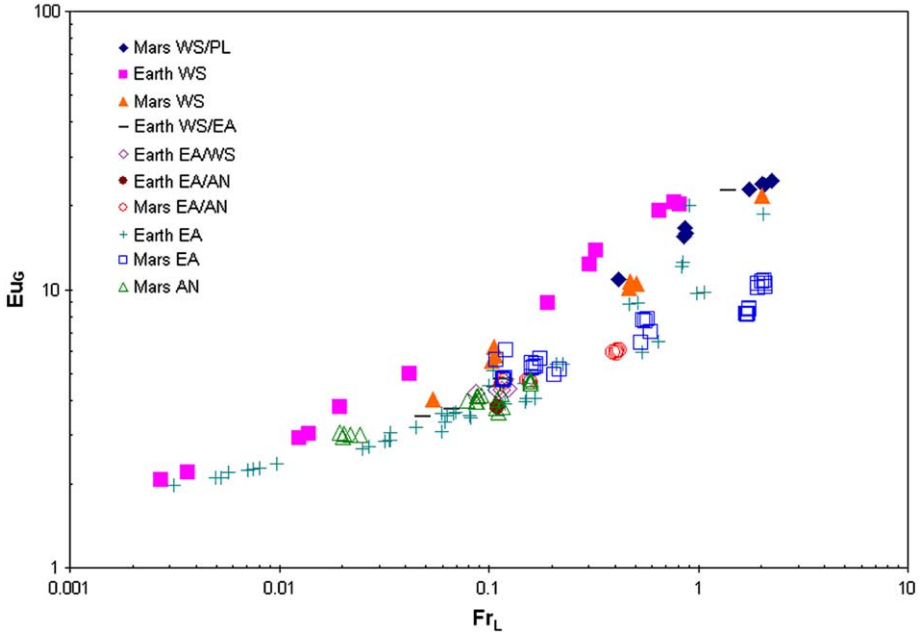

Fig. 6. Eu_G versus Fr_L for 2000 Mars and Earth data with flow regimes specified.

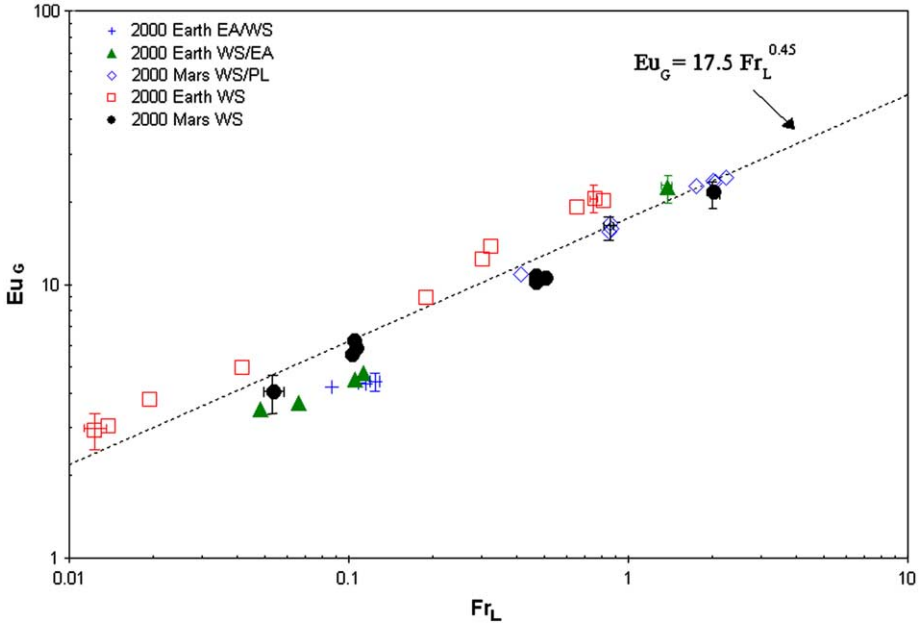

Fig. 7. Eu_G versus Fr_L for 2000 Mars and Earth data for WS and WS-transition flows with $S < 100$.

all basic statistics books, (e.g., Choi, 1978). However, the method does have a major weakness in that it is very sensitive to "outliers" in the data set, which might skew the regression based on

them. However, a Coefficient of Determination allows an assessment of the accuracy of the fitted curve. The formulation is

$$\text{Coefficient of Determination} = 100R^2, \tag{15}$$

where

$$R^2 \approx \frac{\text{total variance of } Y - \text{unexplained variance of } Y}{\text{Total variance of } Y}. \tag{16}$$

The Coefficient of Determination can be interpreted as the percent of the total sample variation of Y that is accounted for by its linear association with X. A quantitative example is that for an R-value of 0.8, the computed R^2-value is 0.64, or 64% of the sample variation for variable Y is accounted for by the linear association with the variable X. The higher the value of R and corresponding R^2-value, the better approximation of the data by the curve fit.

Eq. (14) provides an accurate fit for wavy stratified-type data, with an approximate R^2-value of 0.92. A second-order polynomial fit was also evaluated, but provided little improvement in the accuracy of matching the data.

Because of the limited data set of the current testing, previous Moon- and Mars-g data (Ungar et al., 1994) were included for comparison against the developed scaling theory. Fig. 8 shows the wavy stratified and wavy stratified-transition data for all gravity levels and for $S < 100$ in relation to Eq. (14). The power fit agrees well, further supporting the derived scaling relationship.

From Fig. 6, it is expected that the annular and eccentric annular data will have a different functional scaling relationship than that of the wavy stratified-type flows. Fig. 9 shows the

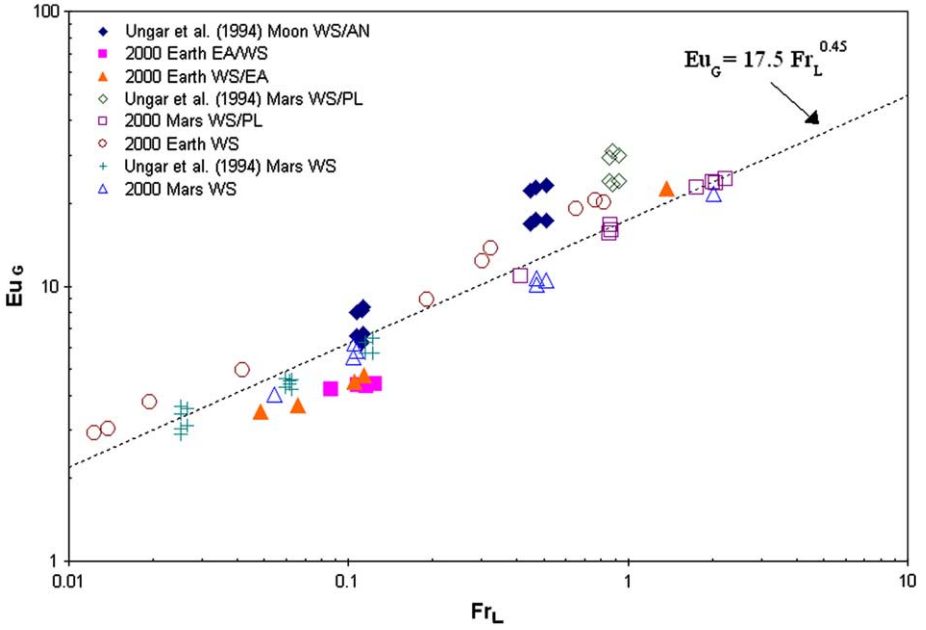

Fig. 8. Eu_G versus Fr_L for 2000 and previous data for WS and WS-transition flows with $S < 100$.

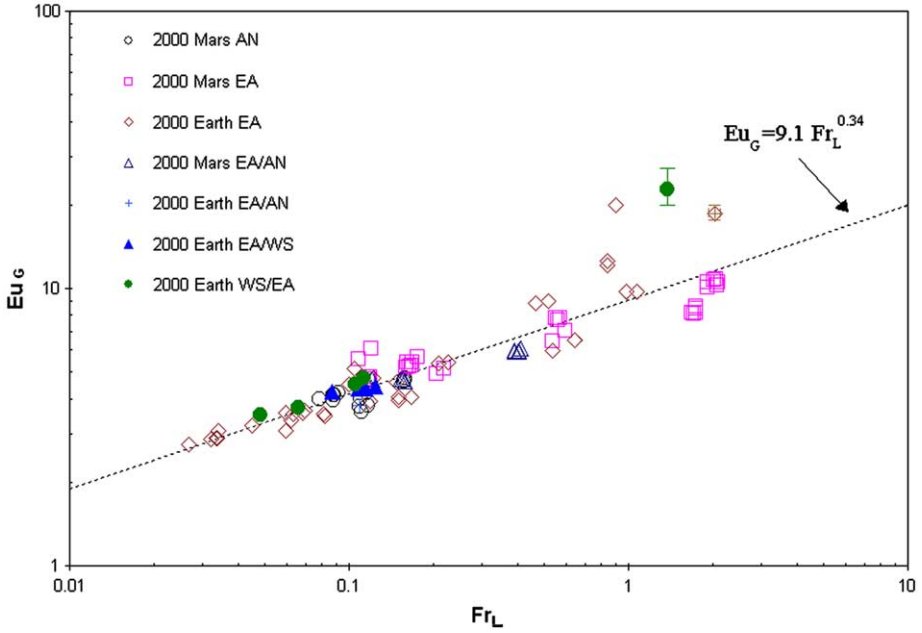

Fig. 9. Eu_G versus Fr_L for 2000 Mars and Earth data for AN and AN-transition flows with $S < 100$.

annular, eccentric annular and associated transition data for the current program, again for $S < 100$.

The best fit of these data yields

$$Eu_G = 9.1 Fr_L^{0.34}. \tag{17}$$

Eq. (17) fits the data with a value of R^2 of approximately 0.64. The lower R^2-value was believed to be at least partly attributable to the limited data set obtained in the current research. Therefore, the earlier data of Ungar et al. (1994) were also used for comparison. Fig. 10 shows all of the annular, eccentric annular and transition data from the current program and from Ungar et al. (1994). The best fit for all of these data is an equation of the form

$$Eu_G = 12.7 Fr_L^{0.41}. \tag{18}$$

Eq. (18) is the curve fit shown in Fig. 10, and has an R^2-value of approximately 0.86. Both Eqs. (14) and (18) match the current and earlier data well, and this supports the scaling approach developed in Section 3.

4.3. Scaling across gravity levels

While the results of this work clearly indicate that scaling across gravity levels using Earth-based testing is possible, a more dramatic result would be determining the specific effect that gravity has on the similarity relationship. If we return to the earlier functional scaling relationship shown in Eq. (11), it is clear that the dimensional pressure drop is only a function of five independent variables,

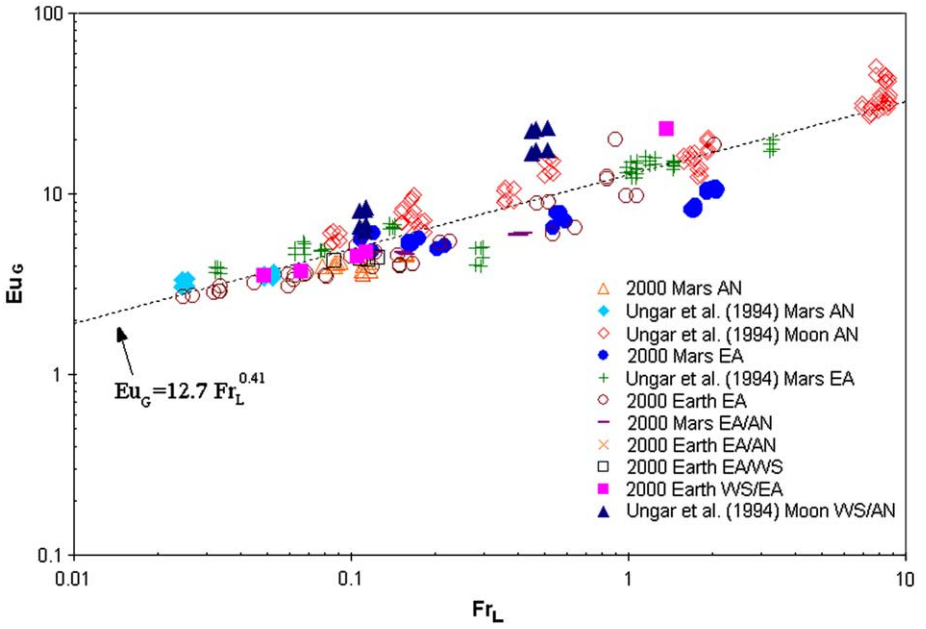

Fig. 10. Eu_G versus Fr_L for 2000 and previous data for AN-type and AN-transition flows with $S < 100$.

$$\Delta p = \mathrm{fn}(j_L, j_G, \rho_G, D, g). \tag{19}$$

In the current research, the fluid properties and D were held approximately constant which simplifies Eq. (19) to

$$\Delta p = \mathrm{fn}(j_L, j_G, g). \tag{20}$$

As described in Section 4.2, the behavior of Eu_G is dependent on the flow regime and the Fr_L. This dependency can be expected for the measured Δp as well. Most of the data for the current research program was for annular-type flows; therefore the analysis in this section is limited to these data.

Plotting the measured test section differential pressure on the ordinate versus the product of the liquid Froude number, gas density and superficial vapor velocity (to the squared power) on the abscissa, Fig. 11 shows a functional relationship for the range of flow conditions across the three gravity levels of this study and the earlier work of Ungar et al. (1994).

A best fit of the distribution of data is shown in the figure, and is represented by the equation,

$$\Delta p = 274(\rho_G j_G^2 Fr_L)^{0.39}. \tag{21}$$

This relationship fits the measured data with an R^2-value of approximately 0.83. The pressure drop relationship of Eq. (21) is a function of j_G, j_L and gravity only, since the geometry and fluid properties were approximately equivalent. For conditions where the superficial velocities are constant, a functional relationship for scaling pressure drop over a range of gravity levels would evolve. This could also be predicted using Eq. (21), where if j_G and j_L were constant, the equation would become

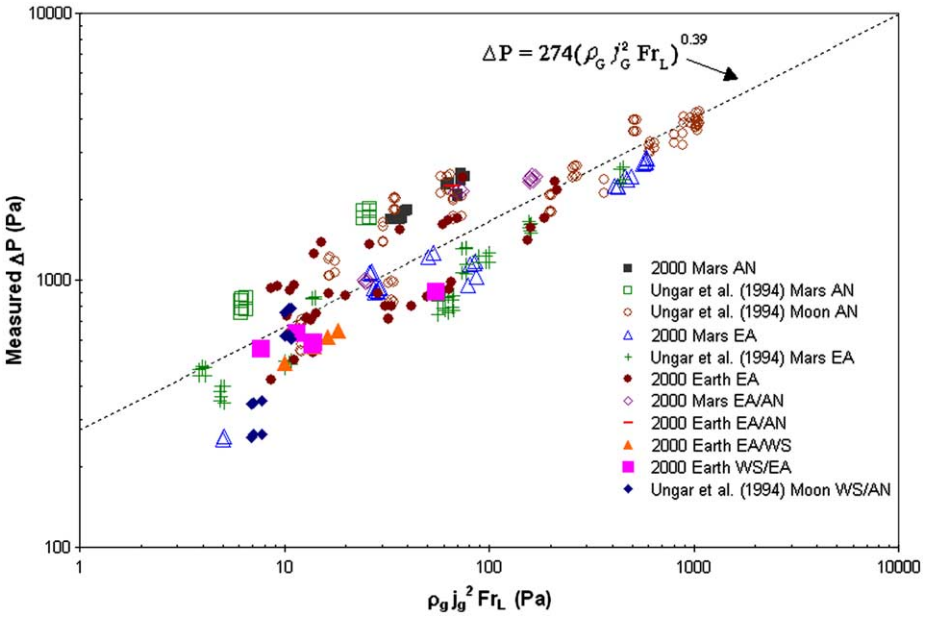

Fig. 11. Measured Δp versus $\rho_G j_G^2 Fr_L$ for 2000 and previous data for AN-type and AN-transition flows with $S < 100$.

$$\frac{\Delta p}{C} = \frac{1}{g^{0.39}}. \tag{22}$$

For Eq. (22), the constant can be empirically determined from Eq. (21) yielding

$$C = 274\left(\frac{\rho_G j_G^2 j_L^2}{D}\right)^{0.39}. \tag{23}$$

To evaluate Eq. (22), the data from the February 2000 flights and the May 2000 ground tests were compared to the earlier Moon data (Ungar et al., 1994) for matching superficial liquid and vapor velocity conditions. Only a limited number of test points were found where j_G and j_L matched within ±5%. Fig. 12 shows a plot of the measured $\Delta p/C$, with C calculated using Eq. (23), versus gravity as well as the fit of Eq. (22). Good agreement is obtained and this supports the functional relationship for annular-type flows,

$$\Delta p_{2\phi} = \mathrm{fn}\left(\frac{1}{g^{0.39}}\right). \tag{24}$$

It should be noted that while Eq. (24) correlates the limited available pressure drop data (for which j_G and j_L agree) reasonably well, it would yield an inconsistent value of Δp as gravity approaches zero. However, Eq. (24) is based on the notion of an inertially controlled mechanism, as represented by Eq. (21). As gravity approaches zero, the ratio of interfacial forces and gravity forces should become more significant, as represented by the Bond number for example. Thus, this effect would have to be accounted for at low gravities. Data at low gravities that match the j_G and j_L conditions on Fig. 12 are not available for such a correlation to be made. Additional

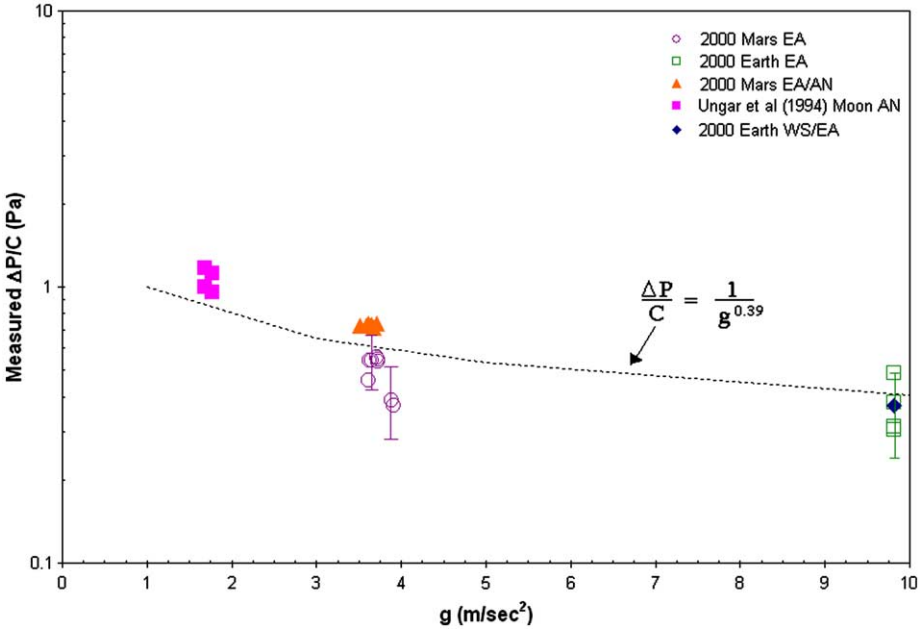

Fig. 12. Measured $\Delta p/C$ versus gravity for 2000 and previous data where the j_G and j_L match to within ±5%.

measurements for near-zero gravities will be required for a proper accounting of the influence of gravity on pressure drop and other pertinent two-phase flow parameters as gravity becomes vanishingly small.

5. Conclusions

Hydrodynamic measurements were made for two-phase flows in Mars, Moon and Earth gravity conditions. A simplified scaling approach was used to develop an expression for scaling Earth-based pressure drop results to obtain values for a Martian or Moon gravity environment for the same working fluid, flow geometry, and two-phase flow pattern. A further result of the scaling study was an evaluation of how the pressure drop varies with gravity. Although a limited amount of data was available, results indicated that the two-phase pressure drop for annular-type flow conditions varies as a function of $1/g^{0.39}$. The research completed supports the use of Earth-g tests to predict the behavior of two-phase systems for Moon-g and Mars-g applications.

References

Choi, S.C., 1978. Introductory Applied Statistics in Science. Prentice-Hall, Englewood Cliffs, NJ.

Crowley, C.J., 1991. Design methods, scaling and microgravity testing of an experimental two-phase thermal system. In: Proceedings of the 4th European Symposium on Space Environmental and Control Systems, Florence, Italy, October 21–24, 1991, paper #ESA SP-324.

Delil, A.A.M., 1991. Thermal gravitational modelling and scaling of two-phase heat transport systems similarity considerations and useful equations predictions versus experimental results. In: Proceedings of the 1st European Symposium Fluids in Space, Ajaccio, France, November 18–22, 1991, pp. 579–599, paper #ESA SP-353.

Delil, A.A.M., 1998. Thermal-gravitational modelling, scaling and flow pattern mapping issues of two-phase heat transport systems. In: Proceedings of the 28th International Conference on Environmental Systems, Danvers, Massachusetts, July 13–16, 1998, paper #NLR TP 98268.

Delil, A.A.M., 1999. Some critical issues in developing two-phase thermal control systems for space. In: 11th International Heat Pipe Conference, Tokyo, Japan, 1999, paper #NLR TP 99354.

Delil, A.A.M., 2000. Thermal-gravitational modelling and scaling of heat transport systems for applications in different gravity environments: super-gravity levels and oscillating heat transfer devices. In: 30th International Conference on Environmental Systems, Toulouse, France, July 10–13, 2000, paper #2000-01-2377.

Hanford, A.J., 1997. Advanced regenerative life support study. Johnson Space Center Document, March 3, 1997, paper #JSC 38672, CTSD-ADV-287.

Hurlbert, K.M., 2000. Flow dynamics for two-phase flows in partial gravities. Doctoral Dissertation, Department of Mechanical Engineering, The University of Houston.

Jayawardena, S.S., Balakotaiah, V., Witte, L.C., 1997. Flow pattern transition maps for microgravity two-phase flows. AIChE Journal 43, 1637–1640.

Miller, K.M., Ungar, E.K., Dzenitis, J.M., Wheeler, M., 1993. Microgravity two-phase pressure drop data in smooth tubing. In: Proceedings of the ASME 1993 Winter Annual Meeting, AMD-Vol. 174/FED-Vol. 175, New Orleans, LA, November 28–December 3, 1993, pp. 37–50.

Reinarts, T.R., 1993. Adiabatic two-phase flow regime data and modeling for zero and reduced (horizontal flow) acceleration fields. Ph.D. Dissertation, Nuclear Engineering Department, Texas A&M University, May 1993.

Reinarts, T.R., Miller, K.M., Best, F.R., 1993. Two-phase flow regimes in smooth tubing in microgravity, Lunar gravity, Martian gravity, and Earth-Normal gravity. In: Proceedings of the ASME 1993 Winter Annual Meeting, AMD-Vol. 174/FED-Vol. 175, New Orleans, LA, November 28–December 3, 1993, pp. 85–103.

Ungar, E.K., 1995. Single phase vs. two-phase active thermal control systems for space applications: a trade study. In: 33st AIAA Aerospace Sciences Meeting & Exhibit, Reno, Nevada, January 9–12, 1995, paper #AIAA-95-0634.

Ungar, E.K., Chen, I.Y., Chan, S.H., 1998. Selection of a gravity insensitive ground test fluid and test configuration to allow simulation of two-phase flow in microgravity. In: Proceedings of the AIAA/ASME Joint Thermophysics and Heat Transfer Conference, HTD-Vol. 357-3, vol. 3, Albuquerque, NM, June 15–18, 1998, pp.71–77.

Ungar, E.K., Miller, K.M., Chen, I.-Y., 1994. Two-phase pressure drop in lunar and martian gravity: experimental data and predictions. In: 1994 ASME Symposium on Gas–Liquid Flows in Fluid Machinery and Devices, ASME Fluids Engineering Conference, Lake Tahoe, Nevada, June 19–23, 1994.

Wheeler, M., 1992. An experimental and analytical study of reduced acceleration two-phase flow frictional pressure drop. Master's Thesis, Nuclear Engineering Department, Texas A&M University, December.

Wheeler, M., Best, F.R., Reinarts, T.R., 1993. An investigation of two-phase flow pressure drops in a reduced acceleration environment. In: Proceedings of the Tenth Space Nuclear Power and Propulsion Symposium, Albuquerque, NM.